OPEN

Response of Liver Metabolic Pathways to Ketogenic Diet and Exercise Are Not Additive

TAI-YU HUANG[1], FELICIA R. GOLDSMITH[1], SCOTT E. FULLER[1,6], JACOB SIMON[1], HEIDI M. BATDORF[1,2,3], MATTHEW C. SCOTT[1], NABIL M. ESSAJEE[1], JOHN M. BROWN[1], DAVID H. BURK[4], CHRISTOPHER D. MORRISON[5], SUSAN J. BURKE[2], J. JASON COLLIER[3], and ROBERT C. NOLAND[1]

[1]Skeletal Muscle Metabolism Laboratory, Pennington Biomedical Research Center, Baton Rouge, LA; [2]Laboratory of Immunogenetics, Pennington Biomedical Research Center, Baton Rouge, LA; [3]Laboratory of Islet Biology and Inflammation, Pennington Biomedical Research Center, Baton Rouge, LA; [4]Cell Biology and Bioimaging Core, Pennington Biomedical Research Center, Baton Rouge, LA; [5]Laboratory of Neurosignaling, Pennington Biomedical Research Center, Baton Rouge, LA; and [6]School of Kinesiology, University of Louisiana at Lafayette, Lafayette, LA

ABSTRACT

HUANG, T.-Y., F. R. GOLDSMITH, S. E. FULLER, J. SIMON, H. M. BATDORF, M. C. SCOTT, N. M. ESSAJEE, J. M. BROWN, D. H. BURK, C. D. MORRISON, S. J. BURKE, J. J. COLLIER, AND R. C. NOLAND. Response of Liver Metabolic Pathways to Ketogenic Diet and Exercise Are Not Additive. *Med. Sci. Sports Exerc.*, Vol. 52, No. 1, pp. 37–48, 2020. **Purpose:** Studies suggest ketogenic diets (KD) produce favorable outcomes (health and exercise performance); however, most rodent studies have used a low-protein KD, which does not reflect the normal- to high-protein KD used by humans. Liver has an important role in ketoadaptation due to its involvement in gluconeogenesis and ketogenesis. This study was designed to test the hypothesis that exercise training (ExTr) while consuming a normal-protein KD (NPKD) would induce additive/synergistic responses in liver metabolic pathways. **Methods:** Lean, healthy male C57BL/6J mice were fed a low-fat control diet (15.9% kcal protein, 11.9% kcal fat, 72.2% kcal carbohydrate) or carbohydrate-deficient NPKD (16.1% protein, 83.9% kcal fat) for 6 wk. After 3 wk on the diet, half were subjected to 3-wk treadmill ExTr (5 $d \cdot wk^{-1}$, 60 $min \cdot d^{-1}$, moderate-vigorous intensity). Upon conclusion, metabolic and endocrine outcomes related to substrate metabolism were tested in liver and pancreas. **Results:** NPKD-fed mice had higher circulating β-hydroxybutyrate and maintained glucose at rest and during exercise. Liver of NPKD-fed mice had lower pyruvate utilization and greater ketogenic potential as evidenced by higher oxidative rates to catabolize lipids (mitochondrial and peroxisomal) and ketogenic amino acids (leucine). ExTr had higher expression of the gluconeogenic gene, *Pck1*, but lower hepatic glycogen, pyruvate oxidation, incomplete fat oxidation, and total pancreas area. Interaction effects between the NPKD and ExTr were observed for intrahepatic triglycerides, as well as genes involved in gluconeogenesis, ketogenesis, mitochondrial fat oxidation, and peroxisomal markers; however, none were additive/synergistic. Rather, in each instance the interaction effects showed the NPKD and ExTr opposed each other. **Conclusions:** An NPKD and an ExTr independently induce shifts in hepatic metabolic pathways, but changes do not seem to be additive/synergistic in healthy mice. **Key Words:** PEROXISOMAL, MITOCHONDRIA, OXIDATION, NORMAL PROTEIN, TRAINING, PANCREAS

Liver has a robust mitochondrial oxidative capacity and accounts for nearly 25% of basal metabolic rate (1). A significant portion of the metabolic capacity of the liver is dedicated to managing substrate availability for the body. In this regard, the liver is unique because it plays a critical role in substrate synthesis (gluconeogenesis, *de novo* lipogenesis, and ketogenesis) while also having a high capacity for substrate storage (glycogen and triglyceride [TAG]). The importance of these hepatic functions becomes particularly evident under conditions with significant shifts in fuel metabolism including exercise, energy deprivation, and the postabsorptive state.

Acute exercise increases mitochondrial respiration, tricarboxylic acid cycle flux, and fat oxidation in liver (2–4). These shifts in hepatic metabolism help support its role in the exercise response to facilitate production of glucose and ketones that can be used by skeletal muscle and heart to meet increased energy demand (5–7). Exercise training (ExTr) can improve hepatic mitochondrial function, increase fat utilization, and reduce hepatic steatosis; however, this has been reported primarily in models of liver disease (8–10), whereas less is known about adaptations in healthy subjects. Identifying strategies that maximize health benefits from ExTr is important for all populations. One such area is modulating diet to optimize the effects of exercise.

Address for correspondence: Robert C. Noland, Ph.D., Pennington Biomedical Research Center, 6400 Perkins Rd, Baton Rouge, LA 70808; E-mail: robert.noland@pbrc.edu.
Submitted for publication April 2019.
Accepted for publication July 2019.

0195-9131/20/5201-0037/0
MEDICINE & SCIENCE IN SPORTS & EXERCISE®

DOI: 10.1249/MSS.0000000000002105

Ketogenic diets (KD) have gained attention in academic and public health fields because reports indicate they impart beneficial health effects including weight loss/maintenance, increased energy expenditure, and improved glycemic control (11–13). They have also become increasingly popular for exercise enthusiasts. A consistent theme of KD is that they contain very low/no carbohydrate and this relative lack of a key macronutrient can induce adaptations akin to states of energy deficit (11,14). When carbohydrate supply is limited and insulin levels are low, gluconeogenic pathways are activated and hepatic mitochondria process fatty acids and certain amino acids to produce ketones. This latter process, known as ketogenesis, spares glucose by providing an alternative fuel source for peripheral tissues (heart, brain, muscle, etc.). Because liver plays an important role in gluconeogenesis and ketogenesis, it is important to know how hepatic metabolic pathways adapt to a KD and how this type of diet impacts exercise adaptations.

The principles of ketoadaptation suggest the body responds to prolonged feeding of a KD by reprogramming metabolic pathways to maximize lipid utilization while sparing use of carbohydrate, which has been theorized to improve athletic performance (15,16). Although this is still a topic of debate, increasing evidence shows prolonged consumption of a KD enhances *in vivo* fatty acid use during exercise and either maintains or improves performance (16,17). These observations are largely derived from RER, which predominantly represents exercising skeletal muscle. Alternatively, there is little information regarding hepatic adaptations under these conditions. Therefore, we tested hepatic substrate metabolism pathways in lean, healthy mice that underwent an ExTr regimen while being fed a KD. Importantly, although KD consistently have a high fat content and very low/no carbohydrate, protein content often varies. The majority of literature testing effects of KD in rodents have used a low-protein KD (11,12,18–20), which is less relevant to the type of KD usually consumed by humans (16,17,21). As such, the KD used in this study contained normal protein content (NPKD) that was matched to the control diet to 1) more closely mimic KD used by humans, and 2) avoid confounding metabolic adaptations that result from protein restriction (20,22,23). Primary goals of this study were to test the interactive effects of a NPKD and ExTr on hepatic cellular energy sensing pathways, mitochondrial content, substrate oxidative capacity (carbohydrate, amino acid, and lipid), peroxisomal capacity, and endocrine parameters that regulate glucose homeostasis including corticosterone and pancreatic hormones. We hypothesized that ExTr and the NPKD diet would have additive effects to expand hepatic oxidative capacity to utilize ketogenic substrates (lipids and ketogenic amino acids), while also remodeling pathways involved in carbohydrate metabolism in liver and pancreas in a manner to spare glucose.

METHODS

Animals

C57BL/6J male mice were ordered from Jackson Laboratories (Stock 000664; Bar Harbor, ME) at 12 wk of age and studied at 20 wk of age. Mice were group-housed at room temperature under a 12:12-h light:dark cycle and allowed *ad libitum* access to food and water. The Pennington Biomedical Research Center has an AALAC-approved Comparative Biology Core facility and veterinary staff that monitor the health of the animals via a sentinel program and daily inspection. All studies were approved by the Institutional Animal Care and Use Committee.

Study Design

Figure 1A illustrates the study design. Two weeks after arrival (14 wk old) body weight was measured and results were used to assign mice into groups that ensured similar body weight before beginning the dietary intervention. Control mice (n = 20) were switched to a matched control diet (TestDiet 5TJS, St. Louis, MO) consisting of 15.9% calories from protein, 11.9% from fat, and 72.2% from carbohydrate. Alternatively, mice in the experimental group (n = 19) were provided a KD with no carbohydrate (NPKD; TestDiet 5TJQ, St. Louis, MO), which provided 16.1% calories from protein (i.e., nearly isocaloric to matched control diet) and 83.9% from fat. Again, these are matched diets, meaning both were configured using the same sources of protein (casein) and lipid (lard, milk fat, and vegetable shortening), whereas carbohydrate (sucrose and maltodextrin) was only present in the matched control diet. Dietary interventions were sustained for 6 wk. After 2.5 wk on the diet, all mice (n = 39) were habituated on an Exer 3/6 treadmill (Columbus Instruments; Columbus, OH) for 3 d. The treadmill was set at 10° incline and the habituation protocol consisted of 5 min stages at 0, 5, 10 $m \cdot min^{-1}$ followed by 2 min at 15 $m \cdot min^{-1}$. All mice responded well to the habituation protocol, so they were randomly assigned to the following groups: control (low fat) sedentary (Con-Sed, n = 11), control (low fat) ExTr (Con-ExTr, n = 9), NPKD sedentary (NPKD-Sed, n = 10), or NPKD ExTr (NPKD-ExTr, n = 9) groups.

ExTr Protocol

The 3-wk training protocol was initiated after 3 wk on the dietary intervention (Fig. 1A). Mice in the ExTr groups were run on a treadmill for 3 wk, 5 $d \cdot wk^{-1}$, 1 $h \cdot d^{-1}$ using a protocol designed to recapitulate a moderate-to-high exercise intensity. Figure 1B shows mice were trained on a treadmill set at 10° incline and each session started with a 5-min warm-up, followed by a step-wise increase in speed until 65 min to ensure mice reached the desired intensity. To account for adaptations in fitness, exercise intensity was increased each week (Fig. 1B). Aversive stimuli (light tapping with a brush, light electrical shock) were used to ensure mice completed each bout. Mice were monitored continuously, and the exercise protocol was well-tolerated as none exhibited signs of exhaustion (no righting reflex and/or acceptance of light electrical shock for >5 s) or injury (awkward gait, foot injury, etc.).

Tissue Harvest

At the end of week 6, tissues were collected 24 h after the last exercise bout and food was removed 3 h before harvest.

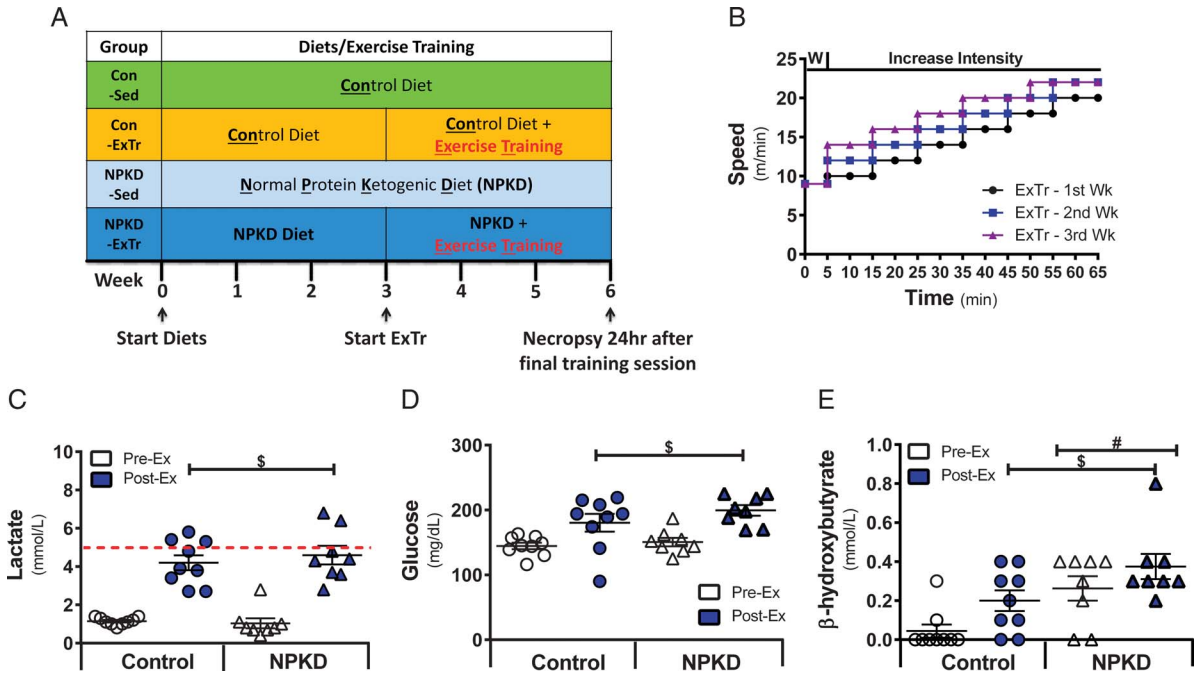

FIGURE 1—Study design and acute exercise responses. Graphical depictions of the overall study design (A) and weekly ExTr protocols (B) are provided. Mice received either a control diet (Con) or a NPKD for 6 wk. Mice were randomly assigned to control sedentary (Con-Sed, *n* = 11), control ExTr (Con-ExTr, *n* = 9), NPKD sedentary (NPKD-Sed, *n* = 10), or NPKD ExTr (NPKD-ExTr, *n* = 9) groups. Mice were trained for 3 wk on a treadmill set at 10° incline and each session started with a 5-min warm-up (W), followed by a progressive increase in speed until 65 min. To account for adaptations in cardiorespiratory fitness, exercise intensity was increased weekly by increasing speed and/or duration of each stage. At the end of week 5, blood lactate (C), glucose (D), and BHB (E) were measured before and immediately after acute exercise. Data are presented as mean ± SEM. #*P* < 0.05 main effect of diet; $ main effect for exercise.

Tissue collection occurred between 9:00 AM and 11:00 AM and mice were anesthetized via i.p. injection of ketamine/xylazine/acepromazine (16 mg·mL^{-1} ketamine, 0.8 mg·mL^{-1} xylazine, and 0.32 mg·mL^{-1} acepromazine delivered at a dose of 0.125 mL/20 g body weight). Trunk blood was obtained via decapitation and allowed to clot at room temperature for 20 min. Serum was then isolated by centrifuging the blood at 2000*g* for 10 min at 4°C and collecting the supernatant. Pancreatic tissue was fixed in neutral-buffered formalin before embedding and sectioning. Liver was collected and either 1) used fresh for substrate oxidation assays, or 2) snap-frozen in liquid nitrogen and stored at −80°C until subsequent analyses could be performed.

Bloodwork

Acute exercise responses for blood glucose (Accu-Chek Aviva Plus Glucometer; Roche Diagnostic, Indianapolis, IN), β-hydroxybutyrate (BHB) (Nova Blood Ketone Monitor; Nova Biomedical, Waltham, MA), and lactate (Lactate Plus Meter; Nova Biomedical, Waltham, MA) were measured via tail vein in conscious mice before and after acute exercise at the end of week 5 (Fig. 1A). Serum lipids were analyzed by measuring non-esterified fatty acids (NEFA) (Wako Chemicals, Richmond, VA) and TAG (Sigma, St. Louis, MO). ELISA kits were used to detect serum insulin (Mercodia, Uppsala, Sweden; Cat 10-1247-01) and serum corticosterone (Enzo Life Sciences, Farmingdale, NY; Cat ADI-900-097). Manufacturer's recommended protocols were used for all measurements.

Liver Substrate Storage

Intrahepatic glycogen and TAG were measured in liver lysates.

Liver glycogen. Roughly 15 to 30 mg of frozen powdered tissue was used to measure glycogen content using a commercially available kit (Abcam ab65620, Cambridge, MA) according to the manufacturer's instructions.

Liver TAG. Roughly 25 to 30 mg of frozen powdered tissue was homogenized 2 × 15 s in 300 µL ice cold 5% NP-40 using a hand-held homogenizer (VWR, Radnor, PA). Tissue homogenates were slowly heated to 95°C in a water bath for 5 min until the solution became white and then cooled at RT for approximately 15 min. This heat-cooling procedure was performed twice to solubilize tissue TAG. Homogenates were centrifuged (14,000*g*, 2 min, RT) and supernatants were collected for liver TAG content determination. A commercially available TAG assay kit (SIGMA® CAT. TR0100) was used to measure glycerol in these extracts as an indirect measure of total TAG. This kit allows for determination of free glycerol, total TAG, and true TAG (total TAG minus free glycerol): all data are reported as true TAG.

Gene Expression

RNA was isolated from frozen powdered liver (~10–15 mg) using an RNeasy kit (Qiagen, Germantown, MD) with proteinase K digestion and on-column DNase treatment, as per the manufacturer's instructions. A Nanodrop ND-1000 spectrophotometer (Thermo Scientific, Wilmington, DE) was used

to measure RNA concentration and quality and 1 μg was used to generate cDNA using an iScript cDNA synthesis kit (Bio-Rad, Hercules, CA). Gene expression was measured by real-time PCR on an ABI 7900HT Sequence Detection System (Life Technologies, Carlsbad, CA) using iTaq Universal SYBR Green Supermix (Biorad; Cat 172-5124). Primer pairs were designed using Primer-BLAST software and gene specificity of primer sequences was initially confirmed computationally via a BLAST search. Primer sequences used for gene expression assays were as follows: Cd36, 5′-GCAAAGAACAGCAGCAAAATC-3′ (forward) and 5′-TCCTCGGGGTCCTGAGTTAT-3′ (reverse); Cpt1α, 5′-TGGTGGTGGGTGTGATATCA-3′ (forward) and 5′-CGCCACTCACGATGTTCTTC-3′ (reverse); CrOT, 5′-CAAGAAGGAGCTGGCAAAAG-3′ (forward) and 5′-GACACGGACCCACAAAGTTC-3′ (reverse); Bhd1, 5′-GATTTGGGTTCTCACTGGCC-3′ (forward) and 5′-TCGGTCACTCTTCAAGCTGT-3′ (reverse); Hmgc1, 5′-AGCAGGTGAAGATCGTGGAA-3′ (forward) and 5′-GGGAGAAACAAAGCTGGTGG-3′ (reverse); Hmgcs2, 5′-GCATAGATACCACCAACGCC-3′ (forward) and 5′-ACTCGGGTAGACTGCAATGT-3′ (reverse); G6Pase, 5′-CGAGGAAAGAAAAAGCCAAC-3′ (forward) and 5′-CAAGGTAGATCCGGGACAGA-3′ (reverse); Fbpase1, 5′-GCATCGCACAGCTCTATGGT-3′ (forward) and 5′-CACAGGTAGCGTAGGACGAC-3′ (reverse); Pck1, 5′-TGTCGGAAGAGGACTTTGAGA-3′ (forward) and 5′-CCACATAGGGCGAGTCTGTC-3′ (reverse); Pex11α, 5′-ACAAAGAGGCCGTGGTACTG-3′ (forward) and 5′-TTGGATGCTCTGCTCAGTTG-3′ (reverse); Pex11β, 5′-CTATGGGCTGGAAAGTCTGG-3′ (forward) and 5′-CTCATAAGCATCACGGCTCA-3′ (reverse); Pex14, 5′-AGCGAGTCTCTCGGAACTGA-3′ (forward) and 5′-ACCTTCTGCTGCTGCTGTCT-3′ (reverse); Pex16, 5′-TACTCTGCCTCGAACCTGCT-3′ (forward) and 5′-CCATGAACACCTCCACACAC-3′ (reverse); Pex19, 5′-GCAAGTCGGAGGCAGTAAGA-3′ (forward) and 5′-TCGCTGCTTTCCAGAAGCTC-3′ (reverse). Other primer sequence information are provided as supplemental Table 2 (10.6084/m9.figshare.7732973) in a previous report (24). Upon arrival, primers were initially screened using a standard curve (triplicate) to ensure proper linearity, whereas melt curves were examined to ensure they were uniform across different standards. mRNA expression was determined using the comparative CT method ($\Delta\Delta C_T$) with an endogenous control (cyclophilin) and converted to a linear function using a base 2 antilog transformation ($2^{-\Delta\Delta CT}$). Data are expressed as fold change compared with the Con-Sed group.

Liver Protein Analysis

Protein lysates were prepared from frozen powdered liver using T-PER buffer (ThermoFisher 78510) containing protease inhibitor cocktail and phosphatase inhibitors from Sigma-Aldrich (St. Louis, MO). Western blot analyses were performed using standard PAGE-SDS as previously described (25). Primary antibodies were as follows: ACC (3676), p-ACC (11818), AMPKα (5831), p-AMPKα (2535), AMPKβ1/2 (4150), p-AMPKβ1 (4181), and Pex5 (83020) from Cell Signaling; Catalase (ab16731), total OXPHOS cocktail (ab110413), Pex19 (ab137072), and PMP70 (ab3421) from Abcam; GLUT2 (07-1402) and Pex14 (ABC-142) from EMD Millipore, and PGC-1α (sc-517380) from Santa Cruz Biotechnology. Horseradish peroxidase-linked secondary antibodies (anti-mouse IgG Cat NXA931 and anti-rabbit IgG Cat NA934V) were purchased from GE Healthcare (Piscataway, NJ) and proteins were detected using enhanced chemiluminescence chemistry. Reversible protein stain-MemCode (MemC) (Thermo-Fisher 24580) was used to confirm equal transfer of proteins and quantitation of these bands served as a loading control. A ChemiDoc imaging system (Bio-Rad) was used to image bands and Image Lab software (Bio-Rad) was used to quantitate band intensity. Data are expressed as fold change compared with the Con-Sed group after normalizing to MemC.

Substrate Oxidation Assays

Liver homogenates were prepared from fresh tissue using a procedure that yields >95% intact mitochondria (24,26–28). Using established methods (26–28), complete substrate oxidation was measured as liberation of $^{14}CO_2$ from homogenates incubated in the presence of [^{14}C]radiolabeled substrates (American Radiolabeled Chemicals, St. Louis, MO) as follows: [1-^{14}C] pyruvate (1 mM) was used to measure pyruvate dehydrogenase (PDH) activity, [2-^{14}C]pyruvate (1 mM) was used to measure pyruvate oxidation, [U-^{14}C]leucine (100 μM) was used to measure oxidation of the branch-chain amino acid leucine, [1-^{14}C]palmitate (200 μM) was used to measure fatty acid oxidation, and [1-^{14}C]lignocerate (25 μM) was used to specifically measure peroxisomal fatty acid oxidation. Incomplete palmitate oxidation was assessed by measuring [^{14}C] acid-soluble metabolite (ASM) formation. Standard liquid scintillation counting was used to measure $^{14}CO_2$ and results were calculated as nanomoles of substrate oxidized per gram tissue wet weight per hour using equations previously reported (27). Results for each substrate (except palmitate) were normalized relative to the average value of the Con-Sed group and are expressed as fold change versus Con-Sed in the paper.

Pancreatic Immunohistochemistry

Using formalin-fixed paraffin embedded pancreatic tissue, 5-μm sections were cut for immunohistochemistry analysis as described (29). Initial analysis was performed using DAB staining to quantify total pancreas area, islet fraction, and insulin positive area. For insulin positive area measurements of immunohistochemistry-stained pancreas sections, whole slide images were analyzed in Visiopharm (Visiopharm, Høsersholm, Denmark) software using custom pipelines to identify pancreas tissue and DAB-positive regions. Islet architecture was examined using primary antibodies for insulin (Abcam ab7842) and glucagon (Cell Signaling 2760). All primary antibody detection was performed using Alexa Fluor secondary conjugation (Alexa 488; Alexa Fluor Plus 555).

Data Analysis

A Shapiro–Wilk normality test was initially performed on all datasets and those that failed to exhibit a normal distribution

were subjected to a Box–Cox transformation. Once a normal distribution was confirmed, a Grubbs test was used to identify outliers. Bloodwork measured before and after acute exercise were analyzed using a two-way repeated measure ANOVA (diet × acute exercise). A two-way ANOVA was used to examine group differences (diet × ExTr). Results from Bonferroni *post hoc* analyses are reported only if interaction effects were observed. GraphPad Prism 5 software (GraphPad Prism Software Inc., San Diego, CA) was used for all statistical analyses and a $P \leq 0.05$ was established *a priori* as representing a statistically significant difference. All data are presented as mean ± SEM.

RESULTS

Study design and acute exercise responses. Mice were weight-matched before the dietary intervention, but upon completion of the study body weight was significantly higher in NPKD-fed mice (in grams): Con-Sed (31.9 ± 1.1), Con-ExTr (30.9 ± 1.1), NPKD-Sed (37.0 ± 1.4), and NPKD-ExTr (34.0 ± 1.4). A sufficient exercise stimulus was confirmed by measuring blood lactate before and after acute exercise (Fig. 1C), which showed mice in both dietary groups achieved postexercise levels that neared the lactate threshold (4–5 mM). Both dietary groups had similar resting blood glucose (fed-state), which increased immediately after the acute exercise bout (Fig. 1D). A rise in blood glucose after acute exercise suggests the rate of appearance (Ra) of glucose exceeded the rate of glucose disappearance (Rd) regardless of the dietary intervention, which is consistent with an exercise protocol that induced a moderate- to vigorous-intensity stimulus that did not approach exhaustion (30,31). These observations are particularly interesting in the NPKD group because this diet had no carbohydrate, which is consistent with the glycogen sparing effects and increased gluconeogenesis that is expected during ketoadaptation (16). Finally, as shown in Figure 1E, not only was there a main effect of diet on circulating BHB, the exercise stimulus also increased BHB (main effect). It is worth noting that BHB after acute exercise in control-fed mice approached levels observed in sedentary NPKD-fed mice (0.20 mM vs 0.26 mM).

AMPK, PGC-1α, and mitochondrial parameters. AMP-activate protein kinases (AMPK) are important sensors of energy status, so we measured total and phosphorylated forms of AMPKα (Figs. 2A and C) and AMPKβ1 (Figs. 2B and C). Total-AMPKα, total-AMPKβ1, and phospho-AMPKβ1 exhibited a main effect due to the NPKD (decrease); however, no alterations were observed in phospho-AMPKα. The ratio of phospho-AMPK to total-AMPK indicated no change in AMPKβ1; however, AMPKα showed significant main effects for both diet (higher) and exercise (lower).

Next, we tested the response of PGC-1α because it is a downstream target of AMPK that plays a role in remodeling numerous metabolic pathways, including mitochondrial dynamics. A main effect of diet was observed for PGC-1α gene (Fig. 2D) and protein (Fig. 2C and E) content, indicating lower PGC-1α in NPKD-fed mice. Exercise training resulted in a main effect on *PGC-1α* gene expression (higher), but this was not observed at the protein level. Although the *PGC-1a* gene was responsive to both diet and ExTr, expression of the mitochondrial transcription factor A (*Tfam*) was only higher in NPKD-fed mice (Fig. 2D). Despite alterations in AMPK and PGC-1α, no differences in electron transport chain complex proteins were observed (Fig. 2C and F). Likewise, few differences were detected in expression of genes involved in mitochondrial fission and fusion (Fig. 2G), with the exception being a main effect of diet on *Opa1* (higher). Overall, these results suggest the NPKD produced inhibitory remodeling of major regulators of energy sensing pathways and substrate metabolism (i.e., AMPK and PGC-1α) in liver. Importantly, although ExTr generally did not override the inhibitory effects of the NPKD on AMPK and PGC-1α, the NPKD did not negatively impact electron transport chain content.

Liver glucose metabolism. Blood glucose at harvest did not differ due to the NPKD or ExTr (24 h after exercise cessation) (Fig. 3A). Again, this is noteworthy because mice in the NPKD group were fed a diet devoid of carbohydrate. Because liver plays a primary role in maintaining glucose homeostasis, we tested if differences in hepatic pathways related to glucose homeostasis were consistent with maintenance of circulating glucose in response to the NPKD and ExTr. Hepatic glycogen reserves displayed main effects of diet and exercise and results point toward both interventions lowering hepatic glycogen (Fig. 3B). We next tested the capacity to utilize carbohydrate as fuel. The NPKD-fed mice had significantly lower PDH activity (Fig. 3C) and pyruvate oxidation (Fig. 3D), whereas ExTr had lower pyruvate oxidation only in mice fed the control diet (Fig. 3D). PDH kinase 4 (Pdk4) is a lipid-responsive gene that moderates a substrate switch that favors lipid utilization to spare glucose; therefore it is surprising that *Pdk4* gene expression was lower in the lipid-enriched, carbohydrate-deficient NPKD groups (main effect) (Fig. 3E). We next tested genes related to gluconeogenesis. Main effects for diet and exercise indicated both NPKD and ExTr groups had lower expression of *G6Pase* (Fig. 3F). Alternatively, *Pck1* was higher after ExTr in control-fed mice, but this was negated in NPKD-fed mice (interaction effect). Finally, neither the NPKD nor ExTr altered GLUT2 protein, which is the predominant glucose transporter in liver (Fig. 3G). Together these findings indicate the liver responds to a NPKD by reducing oxidative capacity to utilize carbohydrate-derived fuels; however, the tissue does not appear to enhance gluconeogenic pathways or increase glycogen storage as a defense to preserve circulating glucose.

Endocrine parameters. Circulating corticosterone did not differ in mice fed a NPKD; however, levels of this glucocorticoid were lower in ExTr mice (Fig. 4A). Similar to blood glucose (Fig. 3A), serum insulin did not differ in either the NPKD or ExTr groups (Fig. 4B). The NPKD mice had significantly smaller islet fraction (Fig. 4D), but the diet appeared to have no impact on total pancreas area (Fig. 4C) or insulin positive area (Fig. 4E). Because previous studies show high-fat and western style diets (high-fat/high sucrose) induce robust

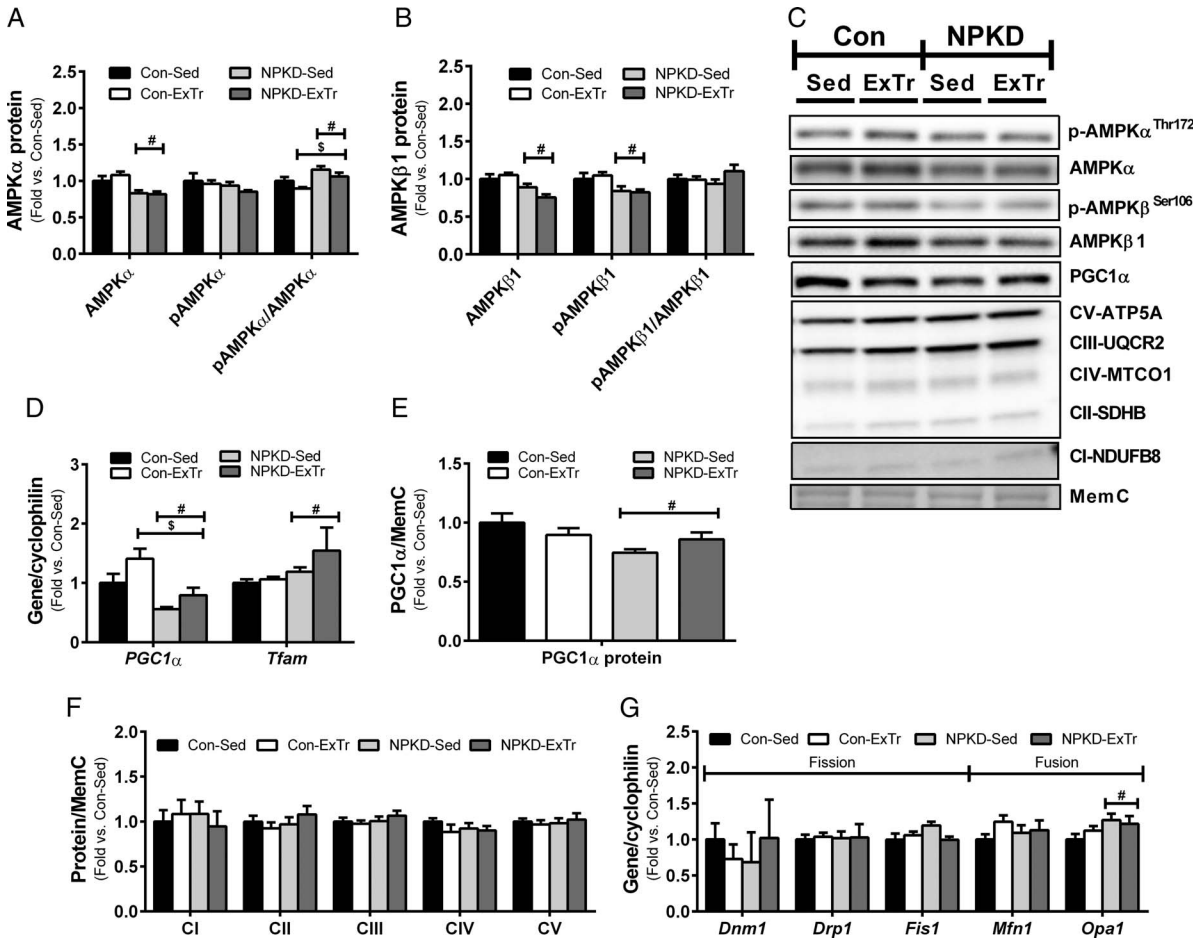

FIGURE 2—AMPK, PGC-1α, and mitochondrial adaptations. Conventional energy sensing protein kinases, AMPKα (A) and AMPKβ1 (B), were measured by Western blotting (WB) using liver protein lysates. Representative images of both AMPKα and AMPKβ1 (phospho- and total) are shown in panel C. Examination of factors involved in mitochondrial biogenesis was tested by measuring expression of *PGC-1α* and *Tfam* gene expression (D) PGC-1α protein (E), protein levels of subunits involved in Complex I-V of the electron transport system (F) and expression of genes involved in mitochondrial fission and fusion (G). Data are presented as mean ± SEM. Quantitated Western blots images and gene expression are normalized to total protein stain using MemCode (MemC) and *cyclophilin* (*PPIB*), respectively. #$P < 0.05$ main effect of diet; $ main effect for exercise.

increases in islet size and insulin positive area (32,33), our data suggest the proliferative response is either driven primarily by carbohydrate content (rather than solely by excess dietary lipid) or by a combination of carbohydrate plus lipid. We note ExTr had no impact on islet fraction (Fig. 4D); however, total pancreas area was lower (Fig. 4C), whereas insulin positive area was higher in ExTr mice (Fig. 4E). These findings are similar to other studies showing ExTr increases islet insulin content (34,35). Immunofluorescent staining for insulin and glucagon show no gross differences in islet architecture amongst any of the interventions (Fig. 4F). Collectively, results indicate mice respond well to both exercise and dietary conditions favoring ketogenesis with no adverse consequences to corticosterone, insulin, or islet morphology.

Fatty acid, amino acid, and ketone metabolism. Because this study utilized a diet that provided 83.9% of energy from fat and 0% energy from carbohydrate, we tested pathways related to lipid metabolism and ketogenesis. Despite substantial dietary lipid, circulating NEFA (Fig. 5A) and TAG (Fig. 5B) were not different due to diet or ExTr. Alternatively, intrahepatic TAG were higher (main effect) in NPKD-fed mice (Fig. 5C). Interestingly, despite the fact that no main effect of ExTr was detected, an interaction effect was observed that showed a pattern for ExTr to increase hepatic TAG in control-fed mice, but decrease TAG in NPKD-fed mice. A lipid-enriched NPKD increased gene expression of a primary plasmalemmal fatty acid transporter, *Cd36*; however, ExTr had no effect (Fig. 5D). Main effects of both NPKD (decreased) and ExTr (increased) were found for the acetyl-CoA carboxylase 1 (*Acc1*) gene (Fig. 5D), whereas only the diet effect (decreased) was observed for total- and phospho-ACC protein (Fig. 5E). Active (unphosphorylated) ACC converts acetyl-CoA to malonyl-CoA, which serves as a precursor for *de novo* lipogenesis and allosterically inhibits mitochondrial lipid entry; therefore, we measured mitochondrial fatty acid oxidative capacity. Data show NPKD-fed mice had higher incomplete palmitate oxidative capacity (Fig. 5F) and expression of key genes (*Cpt1α*, *Cact*, and *Cpt2*) involved in mitochondrial lipid entry (Fig. 5G). Alternatively, ExTr had a main effect showing slightly lower incomplete palmitate oxidation (Fig. 5F). Importantly, incomplete lipid oxidation in liver primarily represents ketone production (36). Because complete oxidation

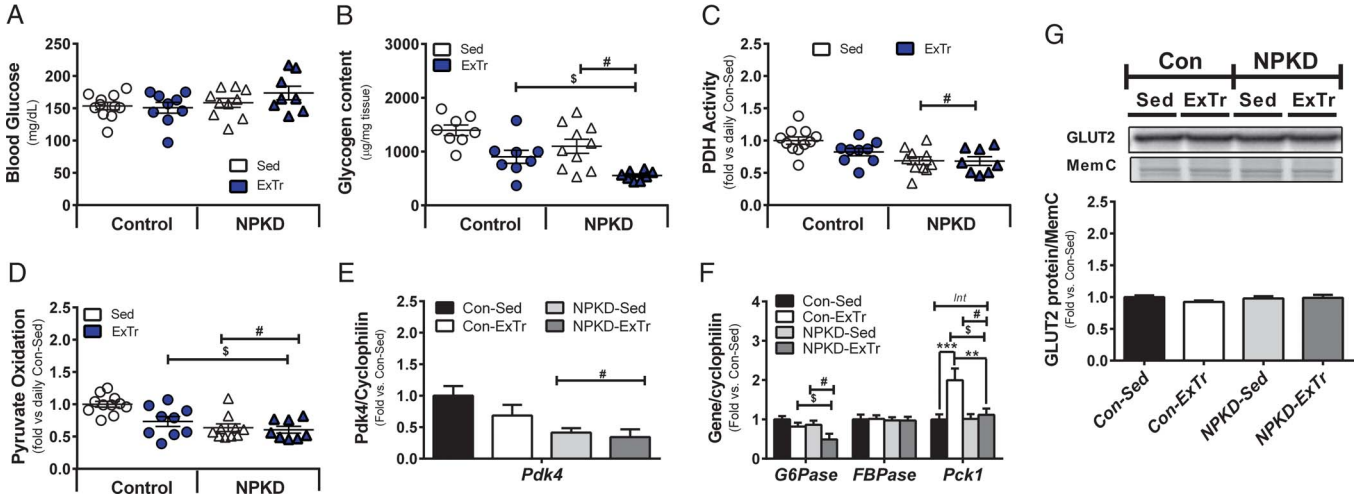

FIGURE 3—Liver glucose metabolism. Adaptations from diet and/or ExTr of liver glucose metabolism were studied by measuring blood glucose (A) and hepatic glycogen content (B) from samples collected at tissue harvest (2–4 h food pull). PDH activity (C) and pyruvate oxidation (D) were measured in liver homogenates. Expression of genes involved in carbohydrate (E) and gluconeogenesis (F) were assessed by RT-PCR. GLUT2 protein was measured by western blot (G). Data are presented as mean ± SEM. RT-PCR data are normalized to *cyclophilin (PPIB)*, whereas protein blots were normalized to total protein stain MemCode (MemC). #$P < 0.05$ main effect of diet; $ main effect for exercise; *Int* Interaction effect; Bonferroni *post hoc* test revealed significant differences (identified with an asterisk) at the following P values $**P < 0.01$; $***P < 0.001$.

(CO_2) did not differ due to diet or exercise, results likely represents a liver with greater ketogenic potential in NPKD-fed mice, whereas this is slightly lower with ExTr.

Although greater hepatic capacity to produce ketones from lipid substrates likely contributes to the higher circulating BHB in the NPKD group (Fig. 1E), ketones can also be derived from certain amino acids. Tyrosine, threonine, isoleucine, phenylalanine, and tryptophan are considered to be both gluconeogenic and ketogenic, whereas lysine and leucine are described as solely ketogenic. With this in mind, leucine oxidation was measured to test hepatic metabolism of a ketogenic amino acid. Consistent with higher ketogenesis, NPKD-fed mice had higher leucine oxidative capacity (Fig. 5H). Alternatively, leucine oxidation was similar in ExTr groups. Differences in leucine oxidative capacity could not be ascribed to regulation of key genes involved in branched-chain amino acid metabolism (Fig. 5I). However, greater ketogenic potential of NPKD-fed mice was supported when measuring key genes involved in ketogenesis (Fig. 5J). ExTr appeared to normalize expression of the D-BHB dehydrogenase 1 (*Bdh1*) gene in NPKD-fed mice, but had no effect on the other ketogenic genes.

Peroxisomal metabolism. Peroxisomes play a critical role in several lipid metabolism pathways, so we assessed peroxisomal adaptations in response to a NPKD and ExTr. Although mitochondria cannot process lipids with a chain length greater than 20 carbons, peroxisomes are uniquely capable of catabolizing very long chain fatty acids. As such, oxidation of lignocerate (C24:0) was used to assess peroxisomal function. As shown in Figure 6A, a main effect indicates peroxisomal oxidative capacity was significantly elevated by the NPKD. Alternatively, ExTr did not alter hepatic peroxisomal fat oxidation (Fig. 6A). The diet-induced increase in peroxisomal oxidation could not be explained by differences in protein levels of key peroxisomal markers (Fig. 6B). Similarly, a main effect of diet was only observed in gene expression of carnitine octanoyltransferase (*CrOT*) and peroxin 16 (*Pex16*), whereas no other peroxisomal genes were specifically altered by the NPKD (Fig. 6C). Interestingly, however, despite the fact that relatively few main effects were observed (diet or exercise), several peroxisomal genes (*CrOT*, *catalase*, *Pex3*, *Pex5*, *Pex11a*, and *Pex11b*) had a significant interaction effect between diet and exercise. Based upon the gene expression pattern, it seems the NPKD alone tended to increase peroxisomal genes; however, the effects of ExTr were to increase peroxisomal genes in control-fed mice, but reduce them in NPKD-fed mice. Overall, results suggest that 1) an NPKD increases peroxisomal fat oxidation, and 2) although moderate- to vigorous-intensity ExTr alone is insufficient to induce peroxisomal remodeling in liver of control-fed mice, ExTr may be capable of normalizing peroxisomal function in NPKD-fed mice.

DISCUSSION

With growing interest in KD as therapeutic and ergogenic aids, it is important to understand how they impact endocrine and metabolic outcomes. Rodents are the most commonly used model in biomedical research because they provide the ability to perform mechanistic examinations that are not feasible in humans. Unfortunately, the vast majority of literature testing the effects of a KD in rodents have used a low-protein KD (11,12,18–20), which does not mirror the normal- to high-protein KD most commonly consumed by humans (16,17,21). Also, most reports using rodents to test exercise adaptations in liver focus on models of metabolic disease, whereas the effects of ExTr in a healthy population have largely been overlooked. As such, the purpose of this study was to test substrate metabolism pathways in lean, healthy mice in response to ExTr while being fed a high-fat, carbohydrate-deficient KD that had normal

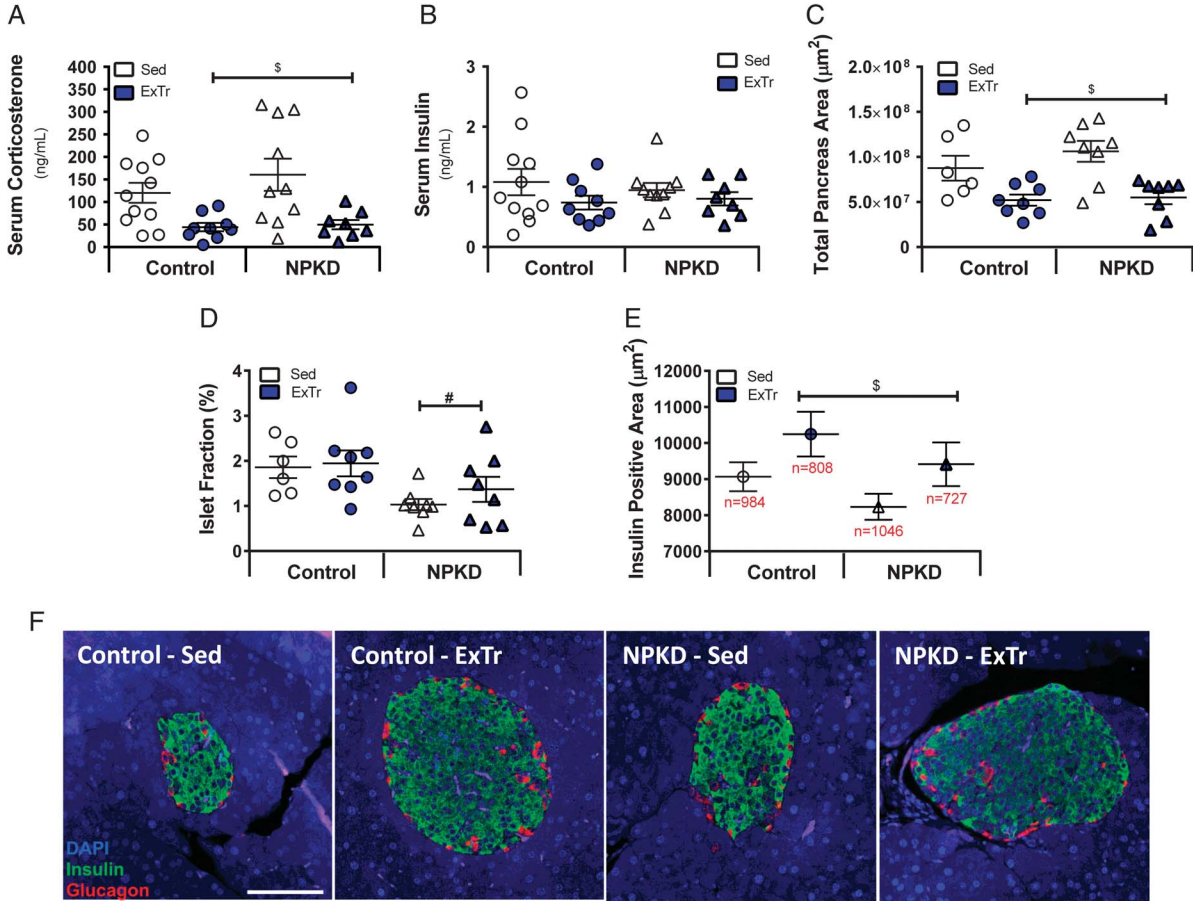

FIGURE 4—Endocrine adaptations to NPKD and ExTr. Serum corticosterone (A) and serum insulin (B) were measured at terminal harvest. Total pancreatic area (C), islet fraction (D), and insulin positive area (E) were measured by immunohistochemistry using DAB staining. Representative islet images show normal islet α-cell and β-cell morphology in response to diet and exercise (F). Scale represents 100 μm. Data are presented as mean ± SEM. #$P < 0.05$ main effect of diet; $ main effect for exercise.

protein content (NPKD). Our primary focus was to test responses in liver due to its role in gluconeogenesis and ketogenesis, but we also examined the pancreas due to its role in regulating glucose homeostasis. To our knowledge, this is the first study to comprehensively test mitochondrial and peroxisomal substrate oxidative capacity (carbohydrate, amino acid, and lipid) in liver of lean, healthy mice in response to ExTr while on a NPKD.

Mice have a robust gluconeogenic capacity, allowing them to process noncarbohydrate carbon sources (chiefly amino acids) to maintain blood glucose under conditions of carbohydrate deficit (37). Results herein support this notion as mice that consumed a carbohydrate-deficient NPKD maintained blood glucose at rest and during strenuous exercise. Feeding a NPKD induced a 6.5-fold increase in circulating BHB, confirming that it drove ketogenesis; however, absolute concentrations (~0.24 mM) are lower than other models of nutritional ketosis, which has been defined as ketones ≥0.5 mM (16). Induction of mild nutritional ketosis in this study is likely due to provision of enough dietary protein to adequately support gluconeogenesis, thus limiting need to mobilize endogenous protein sources. In support, Bielohuby et al. (38) showed that protein content in a KD is an essential determining factor for ketosis in rodents as rats fed a low-protein KD (5.5% energy as protein) had robust nutritional ketosis, whereas those fed a moderate protein KD (11.8% energy as protein) had modest ketogenesis, and those fed a high-protein KD (19.1% energy as protein) had little change in ketones. With this in mind, most rodent studies to date appear to have aimed to maximize nutritional ketosis as they have used a low-protein KD (11,12,18–20). In our view, there are pitfalls to this approach. Low-protein diets (i.e., nonketogenic) alone increase energy expenditure, reduce body weight, and improve glucose homeostasis; however, mechanisms that mediate these benefits do not always overlap with KD in humans. For example, low-protein diets induce FGF21, which imparts health benefits (20,22,39), yet normal- to high-protein KD consumed most commonly by humans do not induce FGF21 in rodents or humans (21,38). In addition, many tissues rely on amino acid consumption to support energetic and other needs (e.g., growth) (40). Thus, maintaining a normal to high level of dietary protein prevents growth deficits, spikes in FGF21, and other metabolic alterations. Nuances, such as protein content in KD, can make it difficult to translate findings from rodents to humans. Results, herein, show that an NPKD-induced mild nutritional ketosis and the adaptations are independent of the effects of protein restriction; therefore, we feel this study offers novel insights relevant to human physiology.

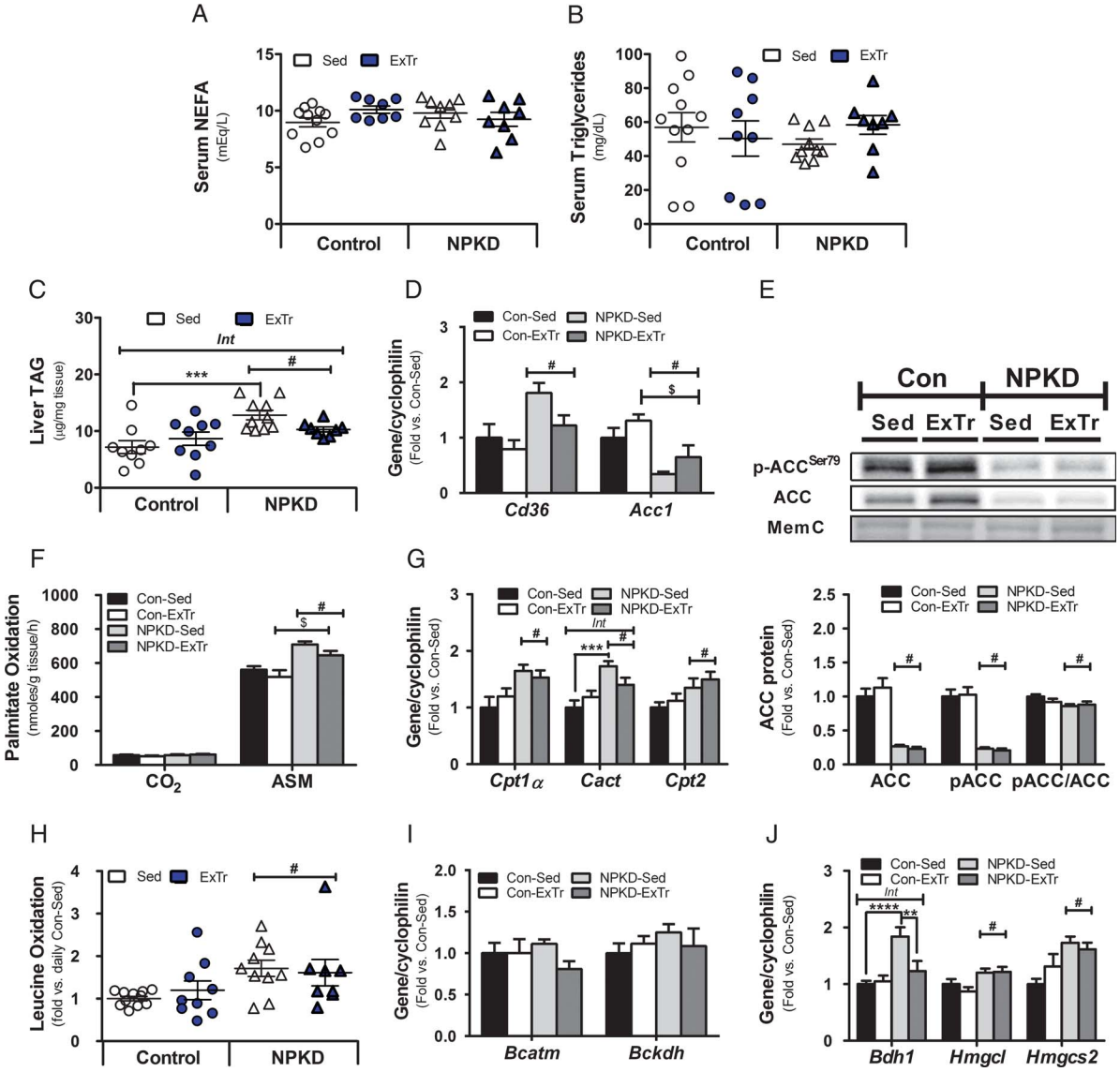

FIGURE 5—Fatty acid, amino acid, and ketone metabolism. Serum NEFA (panel A), and TAG (B) were measured from blood obtained at the time of tissue collection (2–4 h food pull). Parameters related to hepatic lipid storage were tested by measuring liver TAG content (C), expression of *Cd36 and Acc1* genes involved in lipid uptake and storage (D), as well as protein content and phosphorylation status of acetyl-CoA carboxylase (ACC; panel E). Factors related to tissue lipid oxidation were examined by measuring complete (CO_2) and incomplete (ASM) palmitate oxidation (F), as well as expression of genes involved in mitochondrial fatty acid transport (G). Branched chain amino acid metabolism was studied by assessing leucine oxidation (H), as well as expression of the *Bcatm and Bckhd* genes (I). *Bhd1*, *Hmgcl*, and *Hmgcs2* genes (J) were measured as representative genes involved in ketogenesis. Data are presented as mean ± SEM. RT-PCR data were normalized to *cyclophilin (PPIB)*, whereas protein blots were normalized to total protein stain MemCode (MemC). #$P < 0.05$ main effect of diet; $ main effect for exercise; *Int* Interaction effect; Bonferroni *post hoc* test revealed significant differences (identified with an asterisk) at the following P values: **$P < 0.01$; ***$P < 0.001$; ****$P < 0.0001$.

The NPKD actually produced many predicted changes in metabolic pathways in liver that are similar to a low-protein KD, including lower carbohydrate utilization, higher use of a ketogenic amino acid (leucine), and higher lipid utilization (mitochondrial and peroxisomal). Shifts in substrate metabolic capacity in NPKD-fed mice occurred despite a decrease in PGC-1α and no difference in mitochondrial content, which is similar to findings using a low-protein KD (14,19,41). Mice fed the lipid-enriched NPKD had higher intrahepatic TAG, which also seems to occur regardless of the amount of dietary protein (11,12); however, the degree of steatosis observed with KD is likely less than that seen with a traditional high-fat "western" diet (42). In contrast, a notable difference between the NPKD used herein compared with literature using a low-protein KD is the response of AMPK. Studies using a low-protein KD report activation of AMPK (11,14), whereas findings in the present study show lower total and phosphorylated AMPK. These findings are reminiscent of the differential response of FGF21 due to protein content in KD (38). This is perhaps not surprising considering the fact that AMPK and FGF21 are both activated in response to nutritional stress and a carbohydrate-deficient, low-protein KD is almost certain to impose a greater metabolic stress on liver than a NPKD.

Using models of liver disease, researchers have shown that ExTr can increase hepatic oxidative capacity and reduce steatosis

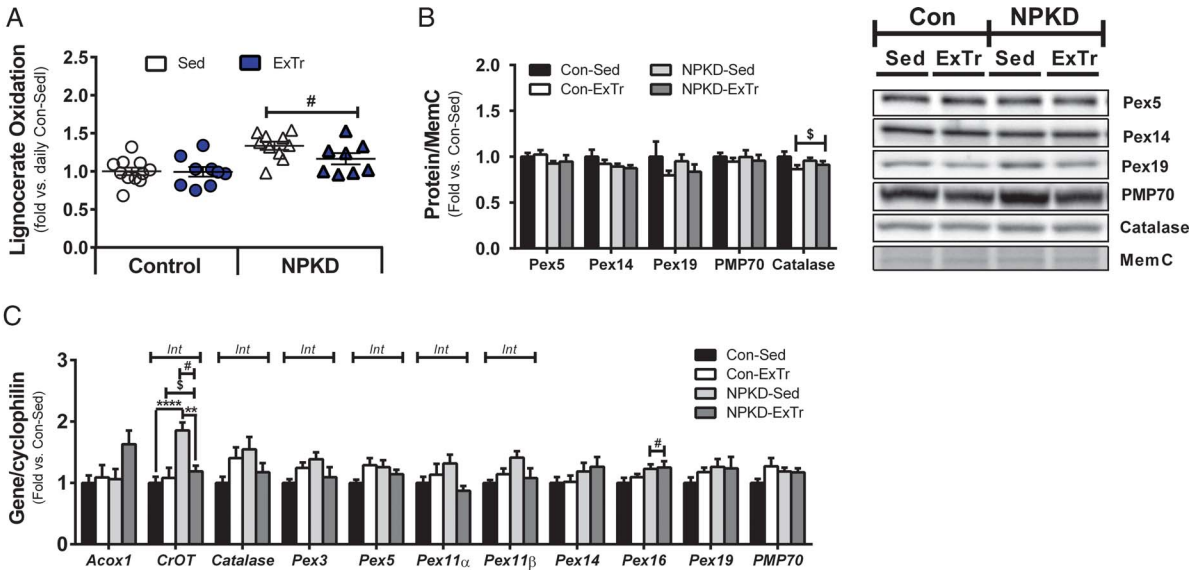

FIGURE 6—Hepatic peroxisomal oxidation is higher in NPKD-fed mice. Peroxisomal fat oxidation was tested by measuring oxidation of the very long chain fatty acid (C24:0), lignocerate (A) in liver homogenates. Peroxisomal proteins (B) and genes (C) were measured and protein images were normalized to total protein using MemCode (MemC), whereas gene expression was normalized to *cyclophilin* (*PPIB*). Data are presented as mean ± SEM. #$P < 0.05$ main effect of diet; $ main effect for exercise; *Int* Interaction effect; Bonferroni *post hoc* test revealed significant differences (identified with an asterisk) at the following P values: **$P < 0.01$; ****$P < 0.0001$.

(8–10); however, less is known about ExTr adaptations in liver of healthy subjects. Results herein indicate that despite the fact that the exercise protocol provided a stimulus sufficient to near the lactate threshold (4–5 mM) and increase circulating BHB to levels similar to a NPKD (i.e., vigorous-intensity), differences in metabolic pathways were not overly robust. PGC-1α is highly involved in adaptations to ExTr as this transcriptional coregulator can increase mitochondrial content (43), enhance peroxisomal biogenesis (25), and is a central modulator of gluconeogenesis (44). *PGC-1α* gene expression was modestly higher in ExTr mice in the present study; however, no evidence of altered mitochondrial or peroxisomal content was observed. Alternatively, ExTr cohorts had lower hepatic glycogen content, pyruvate oxidation, and incomplete palmitate oxidation (ASM), whereas *Pck1* gene expression was higher in mice fed the control diet. Because blood glucose levels were not compromised during exercise, these results may indicate that 1) the liver likely adapted to become more efficient at providing the body with substrates required during exercise (glucose and ketones), and/or 2) the whole organism adapted to more efficiently use lipid as fuel, thus decreasing reliance on carbohydrates (i.e., ketoadaptation). Moreover, there were no major differences in corticosterone, insulin, or islet morphology, showing that the major endocrine factors regulating macronutrient metabolism were largely unperturbed by the dietary and exercise interventions used.

Ketogenesis is traditionally thought of as a response to prolonged fasting that occurs to provide an alternate fuel source to spare glucose when glycogen is depleted. This physiological relationship has led to the common belief that hepatic glycogen content is depleted in response to a KD; however, the NPKD in this study showed a more modest decrease in liver glycogen. In truth, there is a relative paucity of information in the literature to support the notion that KD deplete liver glycogen; therefore, this claim seems to be driven more by popular media, rather than an abundance of scientific evidence. With this in mind, during ketoadaptation, the body adapts to preferentially use fatty acids while sparing glucose (15,16), and our results are consistent with this concept. Second, subjects fed a KD exhibit a glycogen sparing effect during exercise, and the presence of ketones facilitates glycogen recovery after an exercise bout (16,45). Third, after acute exercise that nearly depletes liver glycogen, mice completely restore these reserves within 3 h despite having no access to food (24). Given this robust gluconeogenic potential, mice in this study had ample time (samples collected 24 h after last exercise bout) to restore glycogen despite being provided a carbohydrate-deficient NPKD. Together, these results support the notion that ketoadaptation modulates liver function to protect glycogen reserves, which contradicts the popular notion that KD deplete hepatic glycogen. It is, however, worth noting that due to their inherently high gluconeogenic capacity, mice have lower glycogen stores than rats or humans (37); thus, glycogen would be more rapidly replenished in mice. Also, the NPKD used in this study only induced mild nutritional ketosis; therefore, it is possible that a KD that induces more robust increases in nutritional ketosis would be associated with more severe depletion of liver glycogen. As such, further investigation is likely required to better define the relationship between various KD and hepatic glycogen content, and whether studies using mouse models in this particular area of inquiry translate well to humans.

AMPK and PGC-1α were lower in NPKD-fed mice and levels were not rescued by ExTr. This is somewhat surprising because low-protein KD and ExTr have been reported to increase AMPK and PGC-1α (11,14). With this in mind, it

seems that the metabolic state induced by a NPKD is sufficient to actually limit activation of these energy sensing pathways. Additionally, significant interactions between diet and exercise were observed for liver TAG, as well as genes involved in gluconeogenesis (*Pck1*), ketogenesis (*Bdh1*), mitochondrial fat oxidation (*Cact*), and several peroxisomal markers *(CrOT, Catalase, Pex3, Pex5, Pex11α*, and *Pex11β*); however, none of these interactions suggest an additive/synergistic relationship, as predicted. Rather, in each instance the interaction effects showed that the NPKD and ExTr adaptations were opposing each other. A possible explanation is that ExTr while on a NPKD accelerated ketoadaptation in muscle (and other tissues) to become more reliant on free fatty acids as metabolic fuel, thus requiring less ketogenic and gluconeogenic potential in the liver; however, further studies would be required to validate this contention.

Overall, results from this study suggest the liver likely responds to a NPKD by limiting carbohydrate utilization pathways and increasing ketogenic potential by enhancing utilization of ketogenic substrates (lipid and ketogenic amino acids). Results also suggest that the response of substrate metabolism pathways to a NPKD appear to be similar to those reported in the literature using a low-protein KD, with the notable exception being lower total and phosphorylated AMPK with the NPKD. These results seem to suggest that protein content of a KD may play a role in activation of energy sensing pathways in the liver. Interestingly, despite the fact that ExTr can activate AMPK, the training regimen used in the present study did not override the decrease in AMPK or PGC-1α induced by the NPKD. Additionally, despite findings suggesting that mice exercised at a vigorous-intensity, ExTr alone had minimal impact on most metabolic pathways. In contrast to our hypothesis, ExTr and a NPKD did not appear to exert additive/synergistic remodeling of the hepatic substrate metabolism pathways tested, but instead seemed to counter the effects of each other. Whether these effects can be at least partially attributed to ketoadaptation in other tissues that limit reliance on hepatic gluconeogenesis and/or ketogenesis warrants further study.

LIMITATIONS

C57BL/6J mice were used because they are the most common mouse model in scientific research and are prone to high-fat diet-induced metabolic dysfunction. However, this strain has an inherent deficiency of nicotinamide nucleotide transhydrogenase, which has an important role in peroxide detoxification (46). Also, the ExTr response of C57BL/6J mice is similar to Balb/C mice, but is less robust than Friend leukemia virus B mice (47). As such, we cannot rule out the possibility that responses to NPKD and ExTr may differ in other mouse strains.

A second limitation is that all mice were exercised at the same absolute intensity. With this in mind, mice fed the NPKD were heavier than control-fed mice, so they experienced a greater workload; therefore, it could be argued that NPKD-fed mice exercised at a higher relative intensity. Although we cannot entirely rule out this possibility, the fact that postexercise blood lactate, glucose, and BHB were similar between the dietary groups, and results from the study generally did not reveal many differential responses to ExTr in mice fed the control versus NPKD diets, suggest differences in relative exercise intensity were not likely to be robust.

A third limitation is that although blood lactate was used to gauge exercise intensity, lactate is also an efficient gluconeogenic substrate. As such, it is possible that mice fed a carbohydrate-deficient NPKD converted lactate to glucose faster than control-fed mice. Not only could this alter the interpretation of exercise intensity between groups but it may also help explain how NPKD-fed mice maintained blood glucose throughout exercise despite having modestly lower hepatic glycogen and greater workload. In this regard, however, it is worth noting that inspection of genes involved in gluconeogenesis, pancreatic hormones that regulate glucose, and circulating glucose suggested the inherent gluconeogenic capacity was sufficient to maintain blood glucose during exercise. Future studies using stable isotope tracers would be ideal to address this matter.

The authors thank the Comparative Biology and Animal Metabolism and Behavior Core, as well as the Genomics Core at PBRC for expert technical assistance and support. This work utilized PBRC core facilities (Genomics, and Animal Metabolism and Behavior) that are supported in part by COBRE (NIH 3 P30-GM118430) and NORC (NIH 2P30-DK072476) center grants from the National Institutes of Health. This research was supported by NIH 1R01DK103860 (R. C. N.). F. R. G. and S. E. F. were supported by a T32 fellowship (AT004094).

Authors have no commercial or financial conflicts of interest to report. The results are presented clearly, honestly, and without fabrication, falsification, or inappropriate data manipulation and do not constitute endorsement by the American College of Sports Medicine.

REFERENCES

1. Wang Z, Heshka S, Gallagher D, Boozer CN, Kotler DP, Heymsfield SB. Resting energy expenditure-fat-free mass relationship: new insights provided by body composition modeling. *Am J Physiol Endocrinol Metab*. 2000;279(3):E539–45.
2. Barakat HA, Kasperek GJ, Dohm GL, Tapscott EB, Snider RD. Fatty acid oxidation by liver and muscle preparations of exhaustively exercised rats. *Biochem J*. 1982;208(2):419–24.
3. Bielecki JW, Pawlicka E, Gorski J. Effect of exhaustive exercise on liver mitochondrial function in the rat. *Acta Physiol Pol*. 1988;39(5-6):421–6.
4. Hughey CC, James FD, Bracy DP, et al. Loss of hepatic AMP-activated protein kinase impedes the rate of glycogenolysis but not gluconeogenic fluxes in exercising mice. *J Biol Chem*. 2017;292(49):20125–40.
5. Conti R, Mannucci E, Pessotto P, et al. Selective reversible inhibition of liver carnitine palmitoyl-transferase 1 by teglicar reduces gluconeogenesis and improves glucose homeostasis. *Diabetes*. 2011;60(2):644–51.
6. Dohm GL, Kasperek GJ, Barakat HA. Time course of changes in gluconeogenic enzyme activities during exercise and recovery. *Am J Physiol*. 1985;249(1 Pt 1):E6–11.
7. Wasserman DH, Connolly CC, Pagliassotti MJ. Regulation of hepatic lactate balance during exercise. *Med Sci Sports Exerc*. 1991;23(8):912–9.
8. Kistler KD, Brunt EM, Clark JM, Diehl AM, Sallis JF, Schwimmer JB. Physical activity recommendations, exercise intensity, and histological severity of nonalcoholic fatty liver disease. *Am J Gastroenterol*. 2011;106(3):460–8; quiz 9.

9. Linden MA, Fletcher JA, Morris EM, et al. Treating NAFLD in OLETF rats with vigorous-intensity interval exercise training. *Med Sci Sports Exerc*. 2015;47(3):556–67.
10. Rector RS, Thyfault JP, Morris RT, et al. Daily exercise increases hepatic fatty acid oxidation and prevents steatosis in Otsuka Long–Evans Tokushima fatty rats. *Am J Physiol Gastrointest Liver Physiol*. 2008;294(3):G619–26.
11. Kennedy AR, Pissios P, Otu H, et al. A high-fat, ketogenic diet induces a unique metabolic state in mice. *Am J Physiol Endocrinol Metab*. 2007;292(6):E1724–39.
12. Badman MK, Kennedy AR, Adams AC, Pissios P, Maratos-Flier E. A very low carbohydrate ketogenic diet improves glucose tolerance in ob/ob mice independently of weight loss. *Am J Physiol Endocrinol Metab*. 2009;297(5):E1197–204.
13. Garbow JR, Doherty JM, Schugar RC, et al. Hepatic steatosis, inflammation, and ER stress in mice maintained long term on a very low-carbohydrate ketogenic diet. *Am J Physiol Gastrointest Liver Physiol*. 2011;300(6):G956–67.
14. McDaniel SS, Rensing NR, Thio LL, Yamada KA, Wong M. The ketogenic diet inhibits the mammalian target of rapamycin (mTOR) pathway. *Epilepsia*. 2011;52(3):e7–11.
15. Noland RC. Exercise and regulation of lipid metabolism. *Prog Mol Biol Transl Sci*. 2015;135:39–74.
16. Volek JS, Noakes T, Phinney SD. Rethinking fat as a fuel for endurance exercise. *Eur J Sport Sci*. 2015;15(1):13–20.
17. Zajac A, Poprzecki S, Maszczyk A, Czuba M, Michalczyk M, Zydek G. The effects of a ketogenic diet on exercise metabolism and physical performance in off-road cyclists. *Nutrients*. 2014;6(7):2493–508.
18. Ellenbroek JH, van Dijck L, Töns HA, et al. Long-term ketogenic diet causes glucose intolerance and reduced β- and α-cell mass but no weight loss in mice. *Am J Physiol Endocrinol Metab*. 2014;306(5):E552–8.
19. Hutfles LJ, Wilkins HM, Koppel SJ, et al. A bioenergetics systems evaluation of ketogenic diet liver effects. *Appl Physiol Nutr Metab*. 2017;42(9):955–62.
20. Laeger T, Henagan TM, Albarado DC, et al. FGF21 is an endocrine signal of protein restriction. *J Clin Invest*. 2014;124(9):3913–22.
21. Christodoulides C, Dyson P, Sprecher D, Tsintzas K, Karpe F. Circulating fibroblast growth factor 21 is induced by peroxisome proliferator-activated receptor agonists but not ketosis in man. *J Clin Endocrinol Metab*. 2009;94(9):3594–601.
22. Hill CM, Berthoud HR, Munzberg H, Morrison CD. Homeostatic sensing of dietary protein restriction: a case for FGF21. *Front Neuroendocrinol*. 2018;51:125–31.
23. Solon-Biet SM, McMahon AC, Ballard JW, et al. The ratio of macronutrients, not caloric intake, dictates cardiometabolic health, aging, and longevity in ad libitum-fed mice. *Cell Metab*. 2014;19(3):418–30.
24. Fuller SE, Huang TY, Simon J, et al. Low-intensity exercise induces acute shifts in liver and skeletal muscle substrate metabolism, but not chronic adaptations in tissue oxidative capacity. *J Appl Physiol (1985)*. 2019;127(1):143–56.
25. Huang TY, Zheng D, Houmard JA, Brault JJ, Hickner RC, Cortright RN. Overexpression of PGC-1alpha increases peroxisomal activity and mitochondrial fatty acid oxidation in human primary myotubes. *Am J Physiol Endocrinol Metab*. 2017;312(4):E253–63.
26. Noland RC, Thyfault JP, Henes ST, et al. Artificial selection for high-capacity endurance running is protective against high-fat diet-induced insulin resistance. *Am J Physiol Endocrinol Metab*. 2007;293(1):E31–41.
27. Noland RC, Woodlief TL, Whitfield BR, et al. Peroxisomal-mitochondrial oxidation in a rodent model of obesity-associated insulin resistance. *Am J Physiol Endocrinol Metab*. 2007;293(4):E986–1001.
28. Wicks SE, Vandanmagsar B, Haynie KR, et al. Impaired mitochondrial fat oxidation induces adaptive remodeling of muscle metabolism. *Proc Natl Acad Sci U S A*. 2015;112(25):E3300–9.
29. Burke SJ, Batdorf HM, Eder AE, et al. Oral corticosterone administration reduces insulitis but promotes insulin resistance and Hyperglycemia in male nonobese diabetic mice. *Am J Pathol*. 2017;187(3):614–26.
30. Romijn JA, Coyle EF, Sidossis LS, et al. Regulation of endogenous fat and carbohydrate metabolism in relation to exercise intensity and duration. *Am J Physiol*. 1993;265(3 Pt 1):E380–91.
31. Trefts E, Williams AS, Wasserman DH. Exercise and the regulation of hepatic metabolism. *Prog Mol Biol Transl Sci*. 2015;135:203–25.
32. Ahren J, Ahren B, Wierup N. Increased beta-cell volume in mice fed a high-fat diet: a dynamic study over 12 months. *Islets*. 2010;2(6):353–6.
33. Burke SJ, Batdorf HM, Burk DH, et al. *db/db* mice exhibit features of human type 2 diabetes that are not present in weight-matched C57BL/6J mice fed a western diet. *J Diabetes Res*. 2017;2017:8503754.
34. Huang HH, Farmer K, Windscheffel J, et al. Exercise increases insulin content and basal secretion in pancreatic islets in type 1 diabetic mice. *Exp Diabetes Res*. 2011;2011:481427.
35. Oliveira CA, Paiva MF, Mota CA, et al. Exercise at anaerobic threshold intensity and insulin secretion by isolated pancreatic islets of rats. *Islets*. 2010;2(4):240–6.
36. McGarry JD, Foster DW. Regulation of hepatic fatty acid oxidation and ketone body production. *Annu Rev Biochem*. 1980;49:395–420.
37. Kowalski GM, Bruce CR. The regulation of glucose metabolism: implications and considerations for the assessment of glucose homeostasis in rodents. *Am J Physiol Endocrinol Metab*. 2014;307(10):E859–71.
38. Bielohuby M, Menhofer D, Kirchner H, et al. Induction of ketosis in rats fed low-carbohzydrate, high-fat diets depends on the relative abundance of dietary fat and protein. *Am J Physiol Endocrinol Metab*. 2011;300(1):E65–76.
39. Laeger T, Albarado DC, Burke SJ, et al. Metabolic responses to dietary protein restriction require an increase in FGF21 that is delayed by the absence of GCN2. *Cell Rep*. 2016;16(3):707–16.
40. Neinast MD, Jang C, Hui S, et al. Quantitative analysis of the whole-body metabolic fate of branched-chain amino acids. *Cell Metab*. 2019;29(2):417–29.e4.
41. Kephart WC, Mumford PW, Mao X, et al. The 1-week and 8-month effects of a ketogenic diet or ketone salt supplementation on multi-organ markers of oxidative stress and mitochondrial function in rats. *Nutrients*. 2017;9(9).
42. Holland AM, Kephart WC, Mumford PW, et al. Effects of a ketogenic diet on adipose tissue, liver, and serum biomarkers in sedentary rats and rats that exercised via resisted voluntary wheel running. *Am J Physiol Regul Integr Comp Physiol*. 2016;311(2):R337–51.
43. Morris EM, Meers GM, Booth FW, et al. PGC-1alpha overexpression results in increased hepatic fatty acid oxidation with reduced triacylglycerol accumulation and secretion. *Am J Physiol Gastrointest Liver Physiol*. 2012;303(8):G979–92.
44. Yoon JC, Puigserver P, Chen G, et al. Control of hepatic gluconeogenesis through the transcriptional coactivator PGC-1. *Nature*. 2001; 413(6852):131–8.
45. Holdsworth DA, Cox PJ, Kirk T, Stradling H, Impey SG, Clarke K. A ketone Ester drink increases postexercise muscle glycogen synthesis in humans. *Med Sci Sports Exerc*. 2017;49(9):1789–95.
46. Fisher-Wellman KH, Ryan TE, Smith CD, et al. A direct comparison of metabolic responses to high-fat diet in C57BL/6J and C57BL/6NJ mice. *Diabetes*. 2016;65(11):3249–61.
47. Massett MP, Berk BC. Strain-dependent differences in responses to exercise training in inbred and hybrid mice. *Am J Physiol Regul Integr Comp Physiol*. 2005;288(4):R1006–13.